Research Journal of Recent Sciences _____ ISSN 2277-2502
Vol. **1(8),** 53-63, August **(2012)** *Res.J.Recent Sci.*

Buckling Load Analysis of Oblique Loaded Stainless Steel 316ti Cylindrical Shells with Elliptical Cutout

Shariati Mahmoud[1], Fereidoon Abdolhosein[2] and Akbarpour Amin[3*]
[1]Mechanical Department, Shahrood University of Technology, Shahrood, IRAN
[2]Mechanical Department, Semnan University, Semnan, IRAN
[3]Young Researchers Club, Semnan Branch, Islamic Azad University, Semnan, IRAN

Available online at: www.isca.in
Received 12th June 2012, revised 16th June 2012, accepted 20th June 2012

Abstract

This paper concerns with experimental and numerical studies on buckling of thin-walled cylindrical shells under oblique loading. The buckling loads are obtained from finite element models. Experiments are conducted on several Specimens made of stainless steel 316ti by using an INSTRON 8802 servo-hydraulic machine. Then results are compared. A very good correlation was observed between numerical simulation and experimental results. Investigations on buckling and post-buckling behavior of cylindrical shells with cutout were carried out for shell length (L), shell diameter (D) and cutout position (CP/L ratio). The specimens were constrained by fixtures that design for this result and inserted at both ends, which mimics the fixed boundary condition used in the finite element simulations.

Keywords: Buckling behavior, elliptical cutout, experimental, numerical, oblique loading.

Introduction

Cylindrical shells are frequently used in the manufacturing of aircrafts, missiles, boilers, pipelines, automobiles, and some submarine structures. These structures may experience oblique loads in their longevity and buckle through these loads. Furthermore, these structures usually have disruptions, such as cutouts, which may have destroyer effects on their stability.

Hodge[1-2] discussed various subjects on limit analysis of structures and rotationally symmetric plates and shells. Van Dyke[3] found stress field around a circular hole in a long cylindrical shell subjected to axial force, internal pressure and torsion based on elastic formulation. El Naschie[4] developed an analytical formulation to obtain the buckling load of cracked cylindrical shells. In the following, he obtained approximate results for the local buckling and post buckling behavior of these members under compression loading. Brogan and Almroth[5] nonlinear analysis of cylindrical shells with cutout was carried out and a Robinson[6] comparison on various yield surfaces for thin shells was presented. Tafreshi[7] numerically studied the buckling and post-buckling response of composite cylindrical shells subjected to internal pressure and axial compression loads using Abaqus. She studied the influences of size and orientation of cutouts and found that an increase of internal pressure resulted in an increase in buckling capacity. Shariati and rokhi[8] studied numerically simulation and analysis of steel cylindrical shells with various diameter and length having an elliptical cutout, subjected to axial compression. They investigated examined the influence of the cutout size, cutout angle and the shell aspect ratios L/D and D/t on the pre-buckling, buckling, and post-buckling responses of the cylindrical shells. Haipeng Han et al.[9] studied the effect of dimension and position of square-shaped cutouts in thin and moderately thick walled cylindrical shells of various lengths by nonlinear numerical methods using the ANSYS software. They also compared their results with experimental studies on moderately thick-walled shells. Finally, they developed several parametric relationships based on the analytical and experimental results using the least squares regression method. Dimopoulos[10] studied the buckling behavior of cantilevered shells with opening and stiffening experimentally and numerically. He focuses on shell slenderness as well as opening and stiffening reflecting the main geometric characteristics of wind turbine towers. Komur[11] carried out the buckling analysis on laminated shells with elliptical cutout numerically.

Some investigations regarding oblique loading of tubular members have been carried out even if studies in this area are limited. Estekanchi[12] using the FE approach, examined the elastic buckling load of cracked cylinders under the combined action of internal pressure and axial compression. They conducted a parametric study, using linear Eigenvalue analyses, on cracked cylindrical shells, in order to estimate the effect of crack type, size and orientation on the buckling load. Rahimi and Poursaeidi[13] carried out plastic analysis of cylindrical shells with a circular hole under the effect of end pure moment. Rahimi and Alashti[14] calculated plastic limit load of cylindrical shells with opening subject to combined loading by various finite element methods. Kim and Wierzbicki[15] explored numerically the crush behavior of columns subjected to combined bending and compression, by prescribing both displacements and rotations at the upper end of a cantilever column. Heitzer[16] found plastic limit load of defective pipes

subjected to internal pressure and axial tensile force with the help of nonlinear mathematical programming. Studies by Reyes et al.[17] of thin-walled aluminum extrusions subjected to oblique loading showed that the energy absorption drops drastically by introducing a load angle of 5^0 compared to the axial crushing. This is due to the different collapse modes, as the progressive buckling of axial crushing is a much more energy-absorbing process than bending. The studies also showed that the energy absorption increased by increasing the wall thickness, and this changed the characteristics of the force–displacement curves. A different approach to increase the energy absorption could be to fill the hollow columns with aluminum foam.

In this paper, linear and nonlinear analyses using the Abaqus finite element software, were carried out in order to study the effect of the elliptical cutouts with identical dimensions on the buckling and post-buckling behavior of stainless steel 316Ti cylindrical shells. The shells have different diameters and lengths. Additionally, for several specimens, experimental buckling test was performed using an INSTRON 8802 servo hydraulic machine and the results of experimental tests were compared to numerical results. A very good correlation between experiments and numerical simulations was observed.

Material and Methods

For this study, stainless steel 316ti thin-walled cylindrical shells with various lengths L=150, 250 and 300 mm, and various diameter D=34, 42 and 50 mm were analyzed. An elliptical geometry was selected for cutouts that were created in the specimens.

Furthermore, the thickness of shells was t=1 mm. Figures-1a and 1b show the geometry of the elliptical cutouts. According to this figure, parameter (*a*) shows the size of cutout height and parameter (*b*) shows the size of cutout width. The distance between the center of the cutout and the lower edge of the shell is designated by CP, as shown in figures-1a and 1b. Specimens were nominated as follows: D42-L250-CP125-a-b.

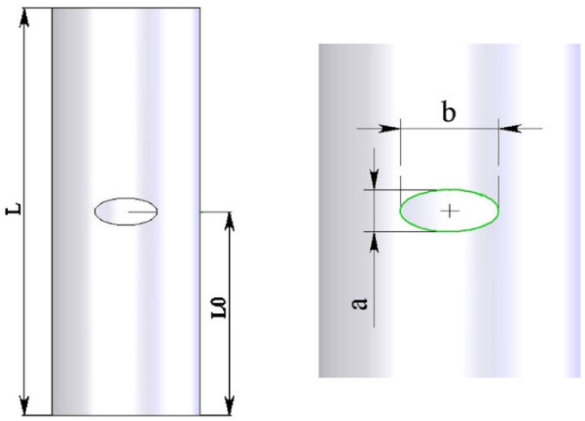

Figure-1
Geometry of cutout

The numbers following D and L show the diameter and length of the specimen, respectively. Parameter γ shows the load angle.

Numerical analysis using the finite element method: The numerical simulations were carried out using the general finite element program Abaqus 6.10-1.

Mechanical properties of the shells: The cylindrical shells used for this study were made of stainless steel 316Ti. The mechanical properties of this steel alloy were determined according to ASTM E8 standard[18] by using the INSTRON 8802 servo hydraulic machine.

The stress-strain curve obtained through tensile test has been shown in figure-2a. Setup test has been shown in figure-2b. Based on the linear portion of stress–strain curve, the value of elasticity module was computed as E=187 GPa and the value of yield stress was obtained as σ_y=334 MPa. Furthermore, the value of Poisson's ratio was assumed to be ϑ=0.33. For more information about true stress–strain curve and plastic property refer to ASTM A370-05[18].

Boundary conditions: In this study, the cylindrical shells were considered as clamped. For applying boundary conditions on the edges of the cylindrical shells, two rigid parts of fixture were used that were attached to the ends of the cylinder.

In order to analyze the buckling subject to combined load similar to what was done in the experiments. 20 mm displacement was applied centrally to the center of the lower rigid base.

Element formulation of the specimens: For this analysis, the nonlinear element S8R5, which is an eight-node element with six degrees of freedom per node, suitable for analysis of thin shells was used[19]. Part of a meshed specimen is shown in figure-3.

Analytical process: To analyze the buckling of cylindrical shells, two analysis methods, linear eigenvalue analysis and geometric nonlinear, were employed using the "Buckle" and "Static-Riks" solvers respectively. For more information about these FE analyses you can refer to Shariati and Mahdizadeh and Abaqus user manual.

Experimental test set-up: Experimental tests using a servo-hydraulic INSTRON 8802 machine were conducted to verify some of the cases investigated in the numerical simulations.

The specimens were constrained by fixtures that design for this result. Fixtures inserted at both ends, which mimics the fixed boundary condition used in the finite element simulations (figure-4).

Results and Discussion

In this section, the results of the buckling analyses of cylindrical shells with elliptical cutouts using the finite element method and experimental method are presented. Comparison of the results

shows that the numerical and experimental methods are well matched.

Results of numerical analysis: Three different shell lengths were analyzed, representing short (L=150 mm), intermediate-length (L=250 m) and long cylindrical shells (L=300 mm). Also three different shell diameters were analyzed, D=34, 42 and 50 mm. Figure-5 shows how oblique loading was realized in the present study. The test specimen was clamped at the upper end. The quasi-static force was applied through a rigid body at the lower end of the specimen. Load angle (γ) is fixed in this study.

The effects of shell lengths (L) on the buckling behavior of cylindrical shells with elliptical cutout: In this section, the results of the buckling analyses of cylindrical shells with elliptical cutouts of different shell length by using the finite element method are presented. Three different shell lengths were analyzed, representing short (L=150 mm), intermediate-length (L=250 mm) and long cylindrical shells (L=300 mm).

Analysis of the effect of change in length (L) of shell with cutout in various height positions of shell on the buckling load: To study the effect of a change in shell length on the buckling load of cylindrical shells, choose shell with different length (L=150, 250 and 300 mm). Then create cutouts with constant size (18×26 mm) in each other at the mid-height position of shells. Then, with changing the cutouts position in L/2 and L/3 of shell height, the change in buckling load was studied. The results of this analysis are presented in table-1.

Buckling capacity of cylindrical shells versus deformation for elliptical cutout with various locations was shown in figures-6 and 7.

Furthermore, buckling load versus shell length produced from the FEM, are shown in figure-8. This figure shows that increasing shell length cause to decrease the shell resistance against buckling. Also this figure shows that decreasing shell length cause to increases the amount of the critical load.

Analysis of the effect of change in position of cutout with constant shell length (L) on the buckling load: Studied the effect of a change in cutout position on the buckling load of cylindrical shells, by created the cutout with constant size (18×26 mm) in the various positions of shells with constant length. With changing the position of the cutouts from CP=L/4 to L/2 mm, the change in buckling load was studied. Figure-9 shows buckling load versus CP/L ratio, by use data from table-1. It can be seen from this figure that when cutout move from mid-height of cylindrical shell to near the shell edge, buckling load increases.

The effects of shell diameter (D) on the buckling behavior of cylindrical shells: In this section, the results of the buckling analysis in cylindrical shells with various diameter (D=34, 42 and 50 mm) contain elliptical cutouts of identical size in different positions using the finite element method were presented. For this purpose, in each diameter a cutout with fixed dimensions was created on the shells with distances from the lower edge of the shell as 0.5L, 0.33L and 0.25L.

Analysis of the effect of change in shell diameter (D) on the buckling behavior of cylindrical shells: In order to analyze the relationship between the buckling load and changes in the diameter, an elliptical cutout with fixed dimension (18×26 mm) was created in the different position of cylindrical shells with various diameter (D=34, 42 and 50). Then the change in buckling load was studied. The results of this analysis are shown in table-2.

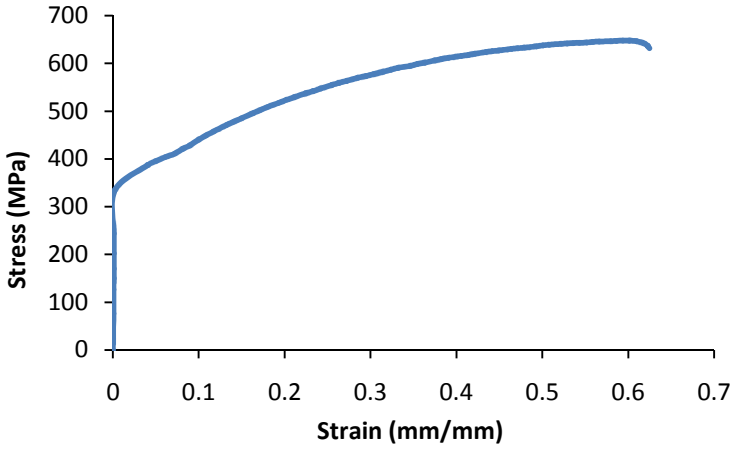

a) Stress–plastic strain curve

b) test setup

Figure-2
Tensile test

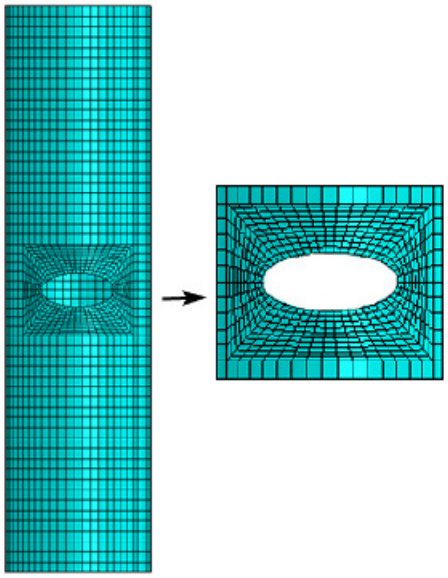

Figure-3
A sample of FEM mesh

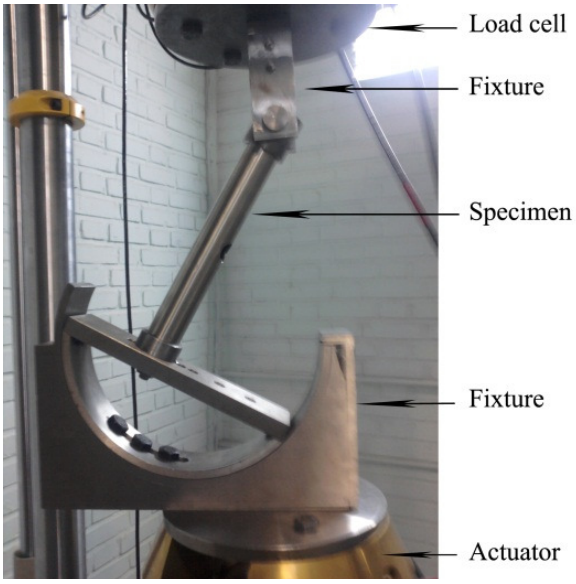

Figure-4
Test setup (INSTRON 8802 machine and special used fixture) with specimen D42-L250-CP125-18-26 before loading (γ=15°)

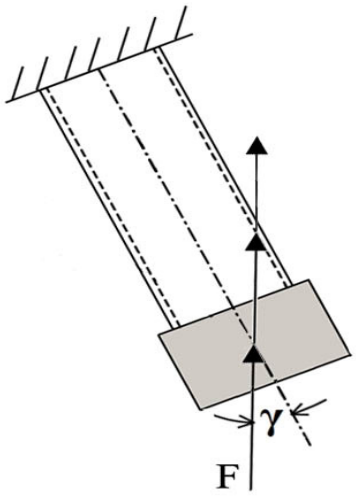

Figure-5
Boundary and loading conditions

Figure-10 shows summary of the buckling capacity of cylindrical shells contain elliptical cutout versus deformation. Figure-11 shows summary of the buckling capacity of cylindrical shells versus deformation for shells contain elliptical cutout. Also this figure shows summary of the buckling capacity of cylindrical shells versus deformation for shell without cutout. The results show that before critical buckling load, with increasing the deformation, buckling load increases. Also results show that after critical buckling load, with increasing the deformation, buckling load decreases. From figure-11, it can be seen that for shell with L=250mm contain cutout in CP=L/2 of shell Length, with change diameter from 34 to 50 the buckling load increases 101%.

The buckling load versus shell diameter with various location of cutout, are shown in figure-12. It is clear that for fixed cutout position, buckling load increases with the increase in the diameter of cylindrical shells. It can be seen that shells with greater diameter have higher buckling loads.

Analysis of the effect of change position of cutout with fixed shell diameter (D) on the buckling load: In order to analyze the relationship between the buckling load and changes in the cutout position, an elliptical cutout with fixed dimension (18×26mm) was created in cylindrical shell with diameter 50 mm. Then with changing the position of the cutouts from mid-height of shell to the near of shell edge, the buckling load was

studied. The buckling Load versus CP/L ratio is shown in figure-13, by use data from table-2. This figure clearly shows that for a cutout with fixed size with changing the position of the cutout from mid-height of the shell toward the edges, the buckling load increases.

Experimental results and verification: Three specimens were tested and almost identical results were obtained compared to those obtained from the numerical simulations[20-24]. The experimental results are compared to numerical findings in table-3. The comparison shows that there is little difference between the two sets of data. The mean difference between the numerical calculations and the experimental results is about 3% of numerical buckling load.

The load-end shortening curves and deformed shape of specimens in the buckling and post-buckling states in numerical and experimental tests are compared in figures-15 and 17. It can be seen that the peak load of both curves are very near together.

Figure-14 shows specimen D42-L250-CP125-18-26 after loading by test setup. Figure-15 shows comparison of deformations resulted by numerical and experimental results by means of oblique loading-Deformation curves and deformed shapes. Figure-16 shows specimen D42-L250-CP125-18-22 after loading by test setup. Figure-17 shows comparison of deformations resulted by numerical and experimental results by means of oblique loading-deformation curves and deformed shapes.

Table-1
Summary of numerical analysis for cylindrical shells with different shell length contain elliptical cutout situated at various locations

Model designation	Shell thickness (mm)	Load angle, γ (degree)	Location of cutout CP/L	Buckling Load (N)
D42-L150-perfect	1	15	-	38810.16
D42-L150-CP125-18-26	1	15	0.5000	33024.83
D42-L150- CP83.3-18-26	1	15	0.3333	33115.73
D42-L150- CP62.5-18-26	1	15	0.2500	33260.08
D42-L250- CP125-18-26	1	15	0.5000	32483.85
D42-L250- CP83.3-18-26	1	15	0.3333	32529.40
D42-L250- CP62.5-18-26	1	15	0.2500	32695.52
D42-L300- CP125-18-26	1	15	0.5000	32272.41
D42-L300- CP83.3-18-26	1	15	0.3333	32391.10
D42-L300- CP62.5-18-26	1	15	0.2500	32498.96

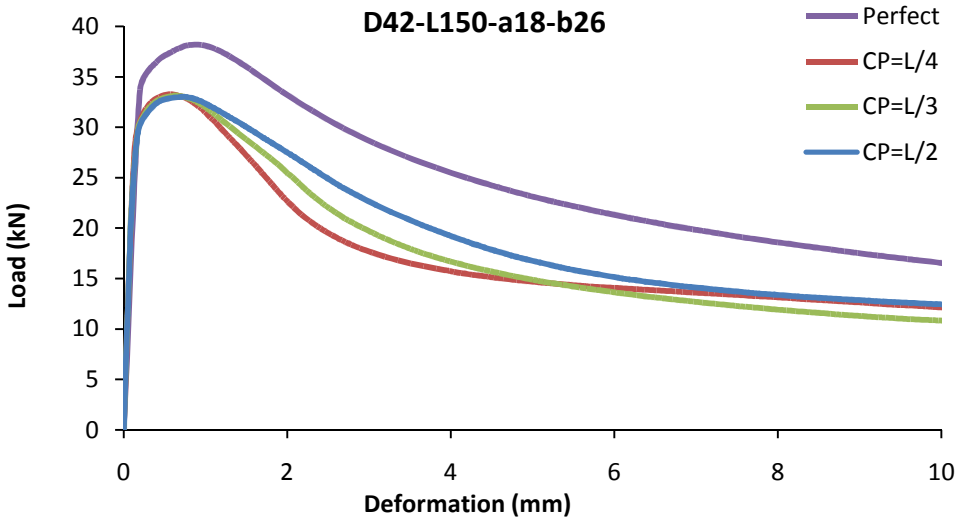

Figure-6
Summary of the buckling capacity of cylindrical shells with elliptical cutout versus deformation, for shell length 150 mm and shell without cut out (γ=15°)

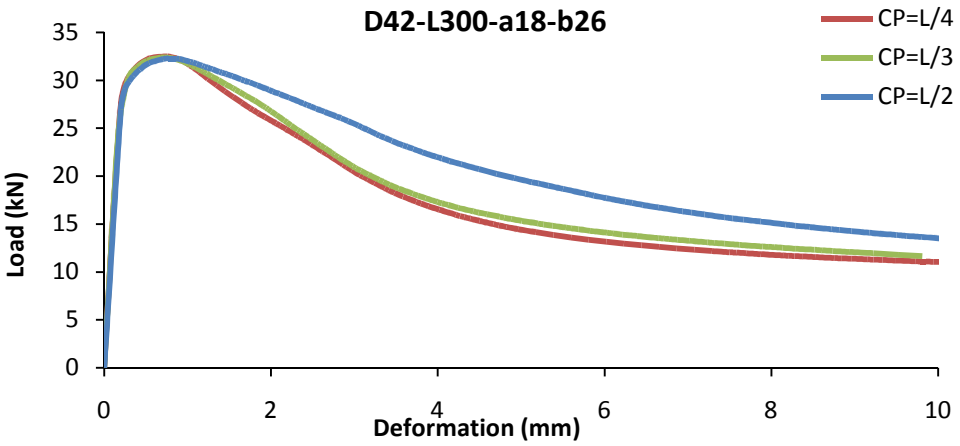

Figure-7

Summary of the buckling capacity of cylindrical shells with elliptical cutout versus deformation, for shell length 300 mm (γ=15º)

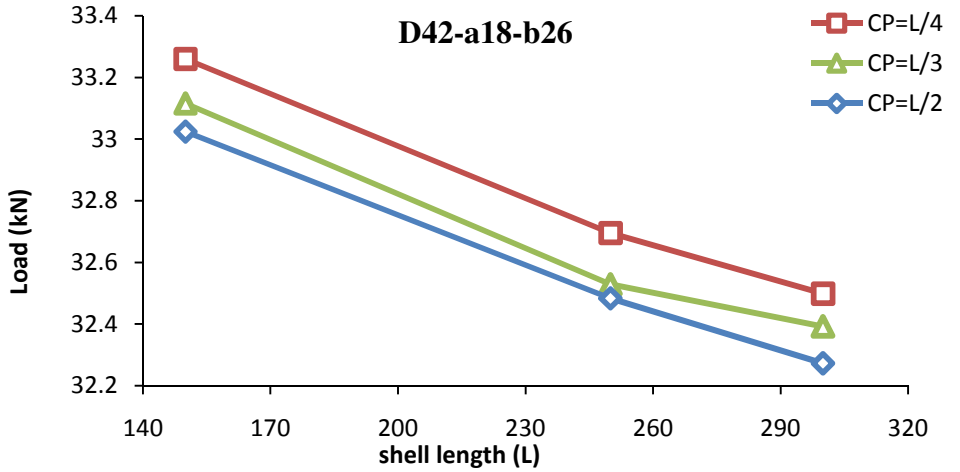

Figure-8

Comparison of the buckling capacity of cylindrical shells versus shell length (L) for various cutout locations (γ=15º)

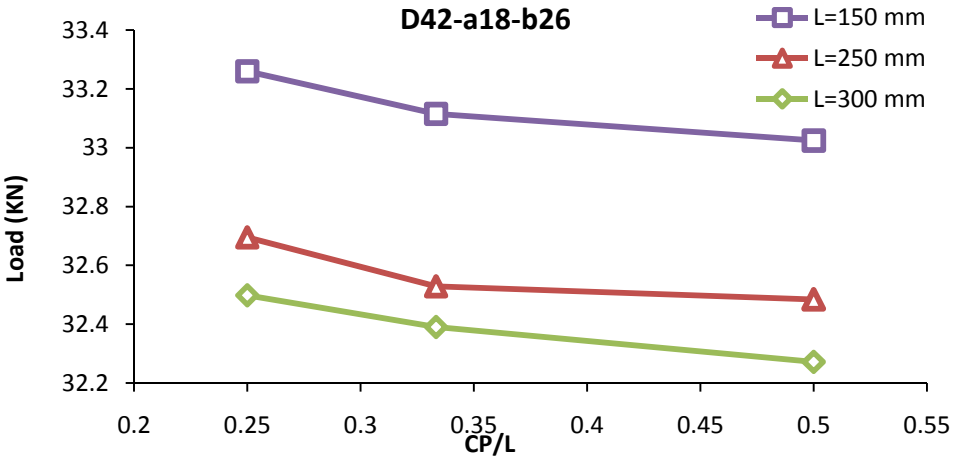

Figure-9

Comparison of the buckling capacity of cylindrical shells versus ratio CP/L, including elliptical cutout in various location (γ=15º)

Table-2
Summary of numerical analysis for cylindrical shells with various cutout angles, with elliptical cutout situated at various locations (γ=15º)

Model designation	Shell thickness (mm)	Load angel, γ (degree)	Location of cutout CP/L	Buckling Load (N)
D34-L250-CP125-18-26	1	15	0.5000	25950.58
D34-L250-CP83.3-18-26	1	15	0.3333	25981.86
D34-L250- CP62.5-18-26	1	15	0.2500	26035.51
D42-L250- CP125-18-26	1	15	0.5000	32483.85
D42-L250- CP83.3-18-26	1	15	0.3333	32573.27
D42-L250- CP62.5-18-26	1	15	0.2500	32715.24
D50-L250-perfect	1	15	-	58726.47
D50-L250- CP125-18-26	1	15	0.5000	52139.38
D50-L250- CP83. 3-18-26	1	15	0.3333	52240.87
D50-L250- CP62.5-18-26	1	15	0.2500	52450.78

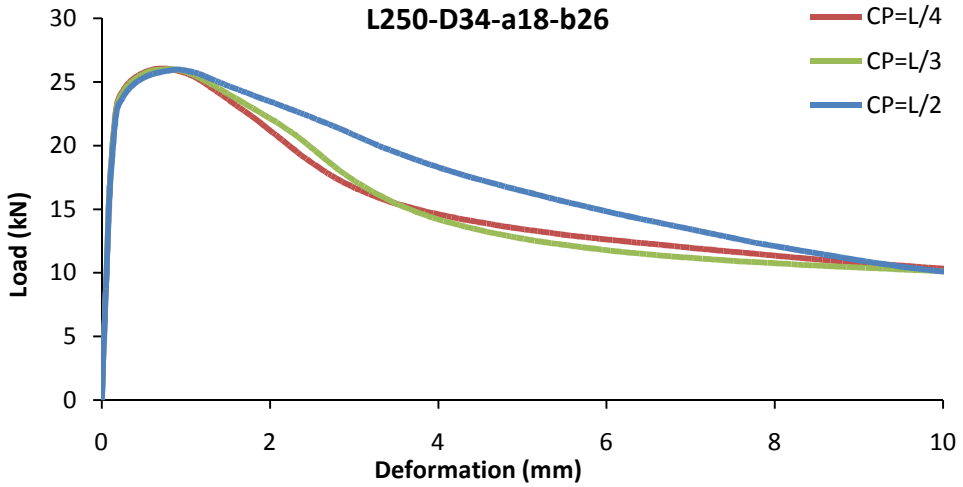

Figure-10
Summary of the buckling capacity of cylindrical shells with diameter 34 mm versus deformation with elliptical cutout (γ=15º)

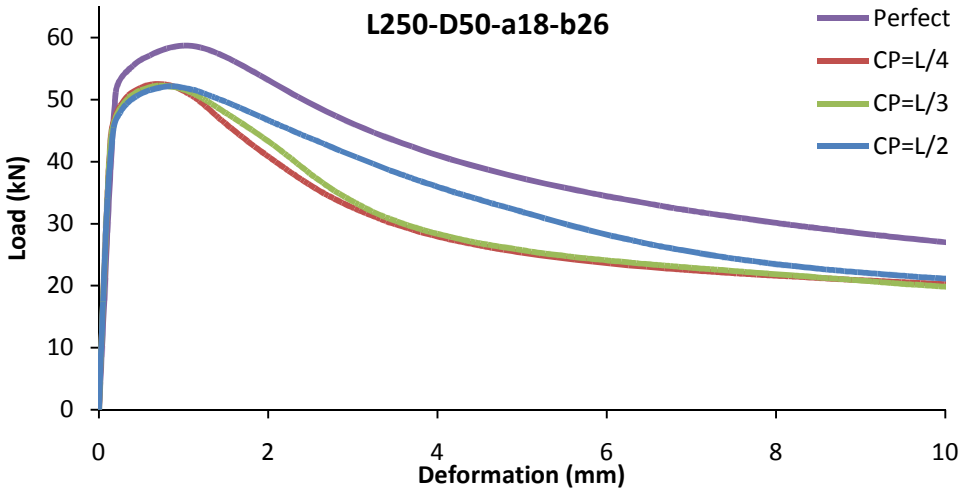

Figure-11
Summary of the buckling capacity of cylindrical shells with diameter 50 mm versus deformation with elliptical cutout, and cylindrical shell without cutout (γ=15º)

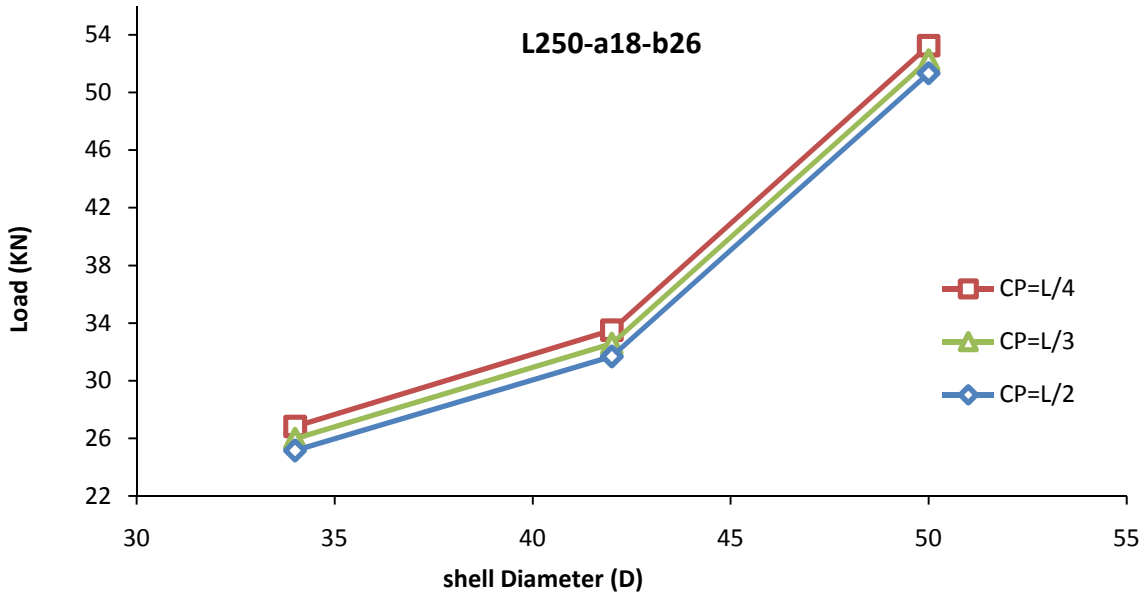

Figure-12
Comparison of the buckling capacity of cylindrical shells versus shell diameter (D) for various cutout locations (γ=15º)

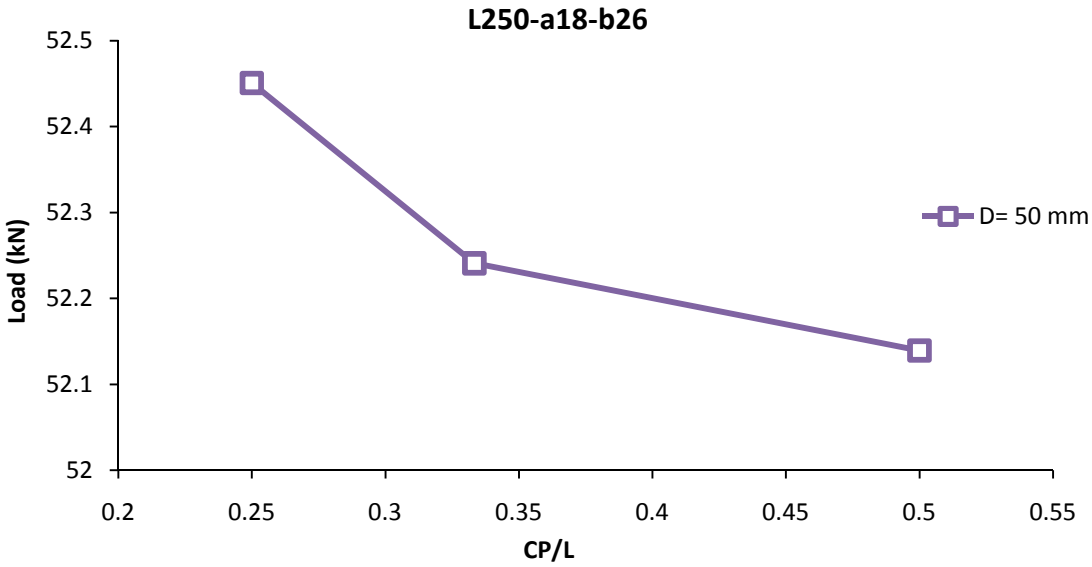

Figure-13
Plot of buckling load versus CP/L ratio for cylindrical shells including an elliptical cutout with various angles (γ=15°)

Table-3
Comparisons of the experimental and numerical results

Model designation	Buckling Load (Experimental) (kN)	Buckling Load (FEM Result) (kN)	Error (%)
D42-L250-CP125-18-26	34.33	33.64	2.1
D42-L250- CP125-18-26	32.77	32.48	1.0
D42-L150- CP125-18-26	35.12	33.02	5.9

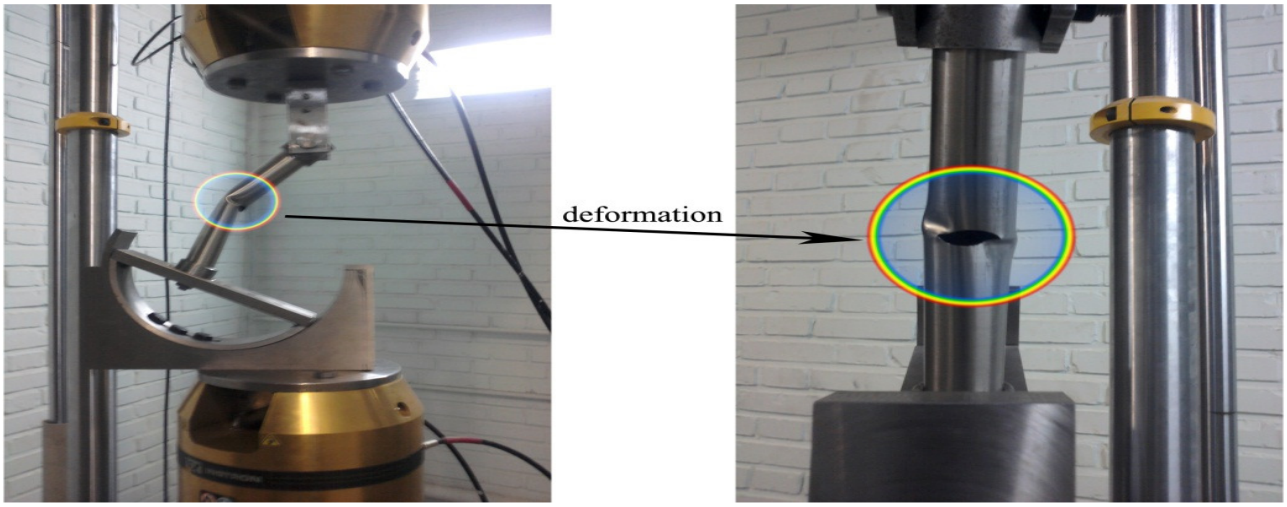

Figure-14
Specimen after loading by test setup on D42-L250-CP125-18-26 (γ=15°)

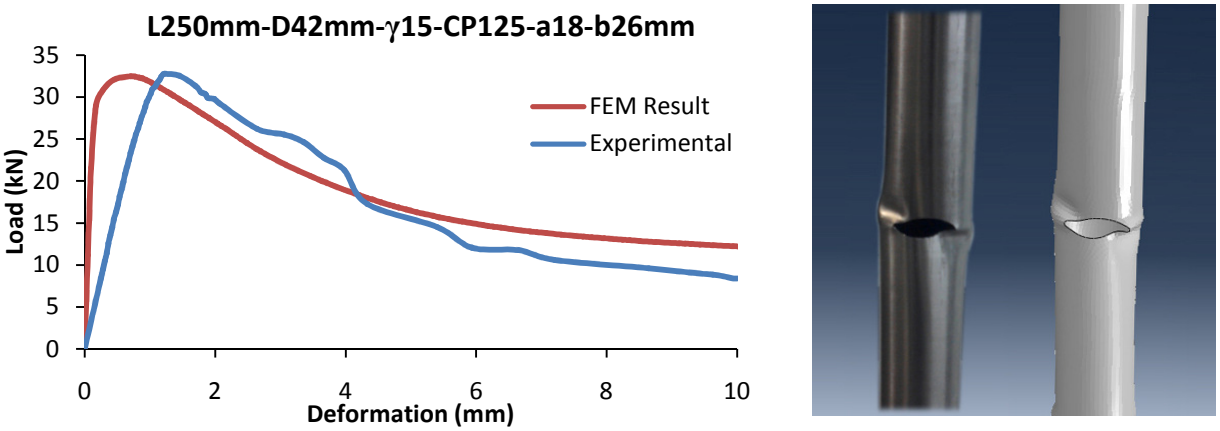

a) loading-deformation curves b) deformed shapes

Figure-15
Comparison of the experimental and numerical results under oblique loading on D42-L250-CP125-18-26 (γ=15°)

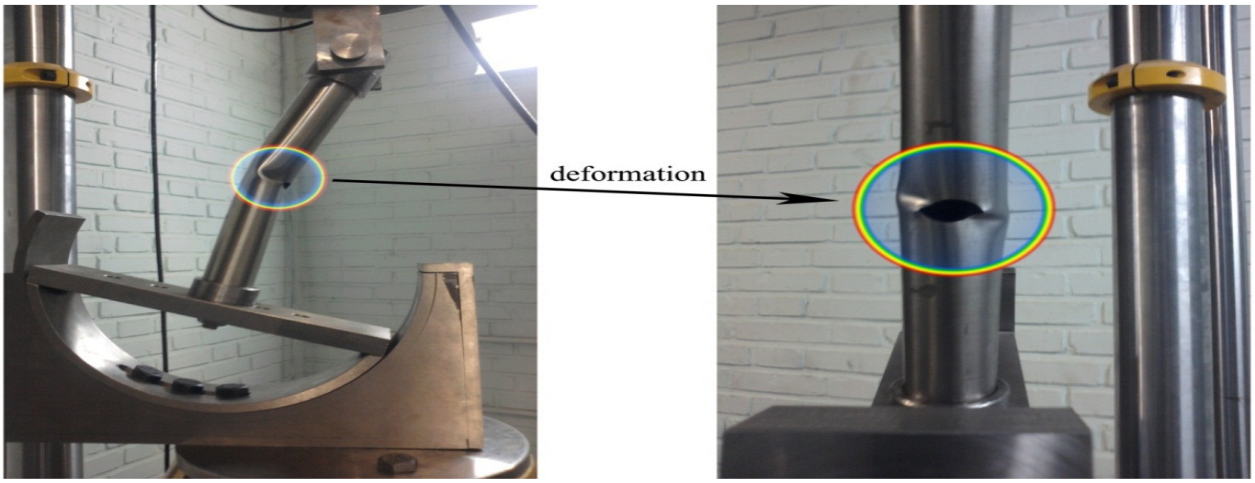

Figure-16
Specimen after loading by test setup on D42-L250-CP125-18-22 (γ=15°)

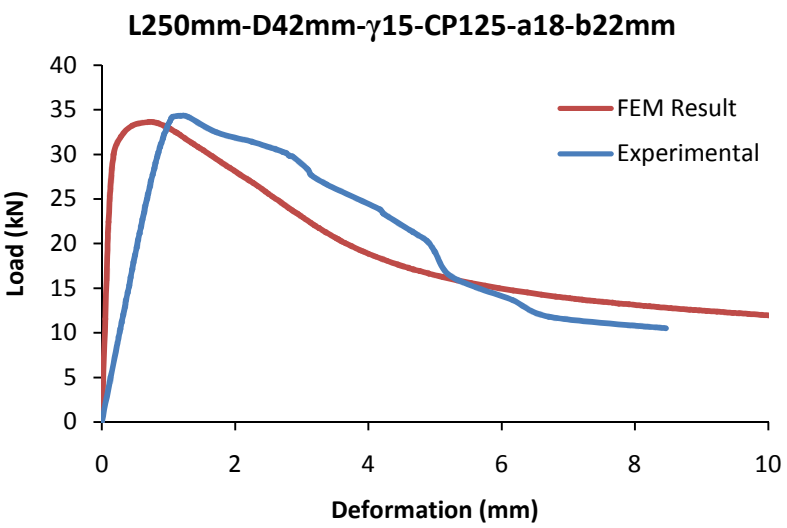

a) loading-deformation curves

b) deformed shapes

Figure-17
Comparison of the experimental and numerical results under oblique loading on D42-L250- CP125-18-22 (γ=15°)

Conclusion

The paper examines the influence of elliptical cutouts of various sizes and angles and various CP/L ratios on the nonlinear response of stainless steel 316ti cylindrical shells subjected to axial compression. To that end, shells with various CP/L ratios were considered. The influence of the size and angle of cutouts at the mid length of the shells was also investigated. Very good correlation was observed between the results of the experimental and numerical simulations. Some results were found in this study. At the first glance, it is fully evident that the presence of the cutout decreases the buckling load capacity of the specimens. Changing the position of the cutout from the mid-height of the shell with constant diameter toward the edges increases the buckling load. When the shell diameter is constant and length of shell increases, the buckling load reduces. Increasing the shell diameter with a fixed thickness increased the buckling load. Also increase in the L/D ratio reduces the buckling load. For cylindrical shells with a cutout, at first the buckling occurs locally, and then the shell experiences general bending. The results show that before critical buckling load, with increasing the deformation, buckling load increases and after critical buckling load, with increasing the deformation, buckling load decreases. Also results show that increasing the diameter of shell while the length is constant, decreases the buckling load extremely.

References

1. Hodge P.G., Plastic analysis of structures, New York: McGraw-Hill Book Company, **(1959)**

2. Hodge PG, Limit analysis of rotationally symmetric plates and shells, Englewood Cliffs, NJ: Prentice-Hall Inc **(1963)**

3. Van Dyke P, Stresses about a circular hole in a cylindrical shell, *AIAA J*, **3(9)**, 1733–42 **(1963)**

4. El Naschie M.S., A branching solution for the local buckling of a circumferentially notched cylindrical shells, *International Journal of Mechanical Sciences*, **16**, 689–697 **(1974)**

5. Brogan A. and Almroth BO., Buckling of cylinders with cutouts, *AIAA J,* **8(2)**, 236–41 (**1970**)

6. Robinson M., A comparison of yield surfaces for thin shells, *Int J Mech Sci*, **13**, 345–54 **(1971)**

7. Tafreshi A., Buckling and post buckling analysis of composite cylindrical shells with cutout subjected to internal pressure and axial compression load, *Int J Pressure Vesssel Piping*, **79**, 351–9 **(2002)**

8. Shariati M. and Rokhi M.M., Buckling of Steel Cylindrical Shells with an Elliptical Cutout. *International Journal of Steel Structures,* **10(2)**, 193-205 **(2010)**

9. Haipeng Han. and Cheng J. and Taheri F. and Pegg N., Numerical and experimental investigations of the response of aluminum cylinders with a cutout subject to axial compression, *Thin-Walled Structure*, 44, 254–70 **(2006)**

10. Dimopoulos C.A., and Gantes C.J., Experimental investigation of buckling of wind turbine tower cylindrical shells with opening and stiffening under bending, *Thin-Walled Structures,* **54**, 140–155 **(2012)**

11. Aydin komur M. et al., Buckling analysis of laminated composite plates with an elliptical/circular cutout using FEM, *Advances in engineering software*, **41**, 161-164 **(2010)**

12. Vaziri, A. and Estekanchi, H.E., Buckling of notched cylindrical thin shells under combined internal pressure and axial compression, *Thin-Walled Structures*, **44**, 141–151 **(2006)**

13. Rahimi G.H. and Poursaeidi E., Plastic analysis of cylindrical shells with single cutout under bending moment. The third international conference on advanced structural engineering and mechanics, Seoul, Korea, 908–22 **(2004)**

14. Rahimi G.H. and Alashti R.A., The plastic limit loads of cylinders with circular opening under combined axial force and bending moment, *J Strain Anal Eng Design*, **42**, 55–66 **(2007)**

15. Kim H. and Wierzbicki T., Crush behavior of thin-walled prismatic columns under combined bending and compression, *Computers and Structure*, **79**, 1417–1432 **(2001)**

16. Heitzer M., Plastic limit loads of defective pipes under combined internal pressure and axial tension, *Int J Mech Sci*, **44**, 1219–24 **(2002)**

17. Reyes, A. and Langseth M. and Hopperstad O.S., Square aluminum tubes subjected to oblique loading, *International Journal of Impact Engineering*, **28**, 1077–1106 **(2003)**

18. ASTM A370-05, Standard test methods and definitions for mechanical testing of steel products **(2005)**

19. ABAQUS 6.10.1 PR11 user's manual **(2012)**

20. Applications of DSTATCOM Using MATLAB/Simulation in Power System Bhattacharya Sourabh, Res. J. Recent Sci., **1(ISC-2011)**, 430-433 **(2012)**

21. Process Parameters Optimization in GFRP Drilling through Integration of Taguchi and Response Surface Methodology Murthy B.R.N., Lewlyn L.R. Rodrigues and Anjaiah Devineni, Res. J. Recent Sci., **1(6)**, 7-15 **(2012)**

22. Numerical Study on Heat Transfer of Internal Combustion Engine Cooling by Extended Fins Using CFD

23. Magarajan U., Thundil karuppa Raj R. and Elango T., *Res. J. Recent Sci.,* **1(6)**, 32-37 **(2012)**

24. Aspect of Finite Element Analysis Methods for Prediction of Fatigue Crack Growth Rate Purkar T. Sanjay and Pathak Sunil, Res. J. Recent Sci., **1(2)**, 85-91 **(2012)**

25. A Finite Element Approach for Analysis of a Multi Leaf Spring using CAE Tools Kumar Krishan and Aggarwal M.L., Res. J. Recent Sci., **1(2)**, 92-96 **(2012)**